

PULMONARY LOW ATTENUATION AREAS ON CT IN ANCA-ASSOCIATED VASCULITIS: A QUANTITATIVE AND SEMI-QUANTITATIVE ANALYSIS CORRELATED WITH PULMONARY FUNCTION TESTING FOR OBSTRUCTIVE AIRWAY DISEASE

Christian W. Cox, Brian J. Bartholmai, Misbah Baqir, Jennifer R. Geske, Ulrich Specks

Department of Radiology, Mayo Clinic Rochester

ABSTRACT. *Objective:* A subset of ANCA-associated vasculitis (AAV) patients are known to manifest obstructive airway disease. Using low attenuation areas (LAA) in the lung on HRCT as an imaging marker for obstructive airway disease, we analyze HRCT studies in AAV patients compared to a matched non-AAV group using visual semi-quantitative and automated quantitative analysis for presence and severity of LAA. Furthermore, HRCT and pulmonary function testing are compared to assess agreement between tests for airway obstruction. *Materials and Methods:* 100 randomly selected AAV patients with HRCT were compared to 100 best-fit matched control subjects. HRCT cases were visually assessed for LAA, along with additional pulmonary patterns. Automated quantitative software analyzed images for texture features and volume of attenuation values of -950 HU or less (e-950). Evidence of obstructive airway disease established by pulmonary function testing, when available, was compared to HRCT analysis for LAA. Additional clinical information, diagnostic testing and mortality data were also compared. *Results:* Both study groups were comprised of 57 females and 43 males with 35 smokers averaging 10.7 pk/yr, with average age for the AAV and control groups being 59.4 yrs and 61.9 yrs, respectively. Visually, 46 AAV patients demonstrated LAA on HRCT compared to 25 control patients ($p=0.0017$) with the difference in LAA presence entirely within the non-smoking subgroup (25 to 3, respectively, $p<0.0001$). Quantitatively, greater than 5% e-950 demonstrated similar significant differences between AAV (36/100) and controls (19/100) ($p=0.0065$), predominantly in non-smokers ($p=0.006$). Obstruction on PFTs was significantly increased in AAV ($p=0.002$) with moderate agreement of obstructive disease with visual LAA on CT (Kappa 0.509). Of the obstructive disease metrics, visual LAA on CT correlated best with mortality ($p=0.0085$). *Conclusion:* Visual LAA and automated quantitative analysis for e-950 on HRCT demonstrate statistically significant increases in AAV patients compared to age, gender and smoking matched controls, with differences primarily seen in the non-smoking subset. AAV revealed statistically significant greater obstructive pulmonary disease on PFTs (*Sarcoidosis Vasc Diffuse Lung Dis* 2020; 37 (4): e2020016)

KEY WORDS: ANCA-associated vasculitis, computed tomography, emphysema, air-trapping, fibrosis

Abbreviations:

AAV- Anti-Neutrophilic Cytoplasmic Autoantibody (ANCA)-associated vasculitis
MPO- Myeloperoxidase

PR3- Proteinase 3
MPA- Microscopic polyangiitis
EGPA- Eosinophilic Granulomatosis with polyangiitis
V-LAA- Visual low attenuation areas
Q-LAA- Quantitative low attenuation areas
UIP- Usual Interstitial Pneumonia
CALIPER- Computer-Aided Lung Informatics for Pathology Evaluation and Rating
PFT- Pulmonary Function Test

Received: 20 April 2020

Accepted after revision: 2 December 2020

Correspondence: Christian W. Cox MD

*200 First Street SW, Rochester MN 55905

E-mail: cox.christian@mayo.edu

INTRODUCTION

Anti-Neutrophilic Cytoplasmic Autoantibody (ANCA)-associated vasculitis (AAV) is an umbrella term used for a group of systemic autoimmune syndromes characterized by necrotizing inflammation of small vessels and the presence of ANCAs targeting either myeloperoxidase (MPO) or proteinase 3 (PR3) (1). AAV comprises microscopic polyangiitis (MPA), granulomatosis with polyangiitis (GPA) and eosinophilic granulomatosis with polyangiitis (EGPA or Churg-Strauss) (2). A recent International Consensus Statement supports immunoassay testing for PR3-ANCA and MPO-ANCA as a primary screening tool for MPA and GPA (3).

Respiratory tract manifestations are a common clinical presentation of AAV; the most common in GPA patients and present in up to a third of MPA patients (4). While upper respiratory involvement with sinusitis is most common, lower respiratory tract manifestations of AAV range from subglottic stenosis to diffuse alveolar hemorrhage. When strictly examining thoracic computed tomography (CT) manifestations of AAV, imaging findings most often include pulmonary nodules/masses, consolidation, cavitation, tracheobronchial wall thickening and bronchiectasis (5,6), although this varies by subtype. More recent imaging based studies have identified an association of MPA and pulmonary fibrosis (7-12).

In our practice, we have recognized sporadic non-smoking AAV patients with CT evidence of multifocal hyperlucent changes of the lung, commonly tracking along the bronchovascular bundles, with features suggestive of emphysema, cysts and/or mosaic attenuation. (Figure 1) Particular types of small vessel vasculitides other than GPA or MPA have a well-recognized association with small airway obstruction. Asthma is a disease-defining feature of EGPA, and hypocplementemic urticarial vasculitis can be associated with basilar predominant panacinar emphysema similar to alpha-1 antitrypsin deficiency disease along with the urticarial skin manifestations (13). In the setting of GPA and MPA, obstructive lung disease and associated imaging changes have been described in a few isolated case reports, small case series and general imaging studies (9,13-16). However, we are unaware of any literature specifically studying hyperlucent or low-attenuation area (LAA) changes on HRCT in pa-

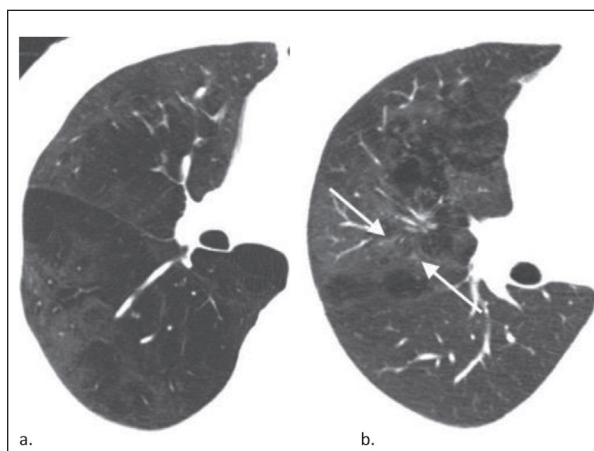


Fig. 1. 42-year-old male (a) and 26-year-old male (b), both non-smokers with PR3 positive ANCA associated vasculitis. Select axial HRCT images in lung window demonstrate low attenuation areas tracking along bronchovascular bundles. Additional ground-glass surrounds regions of LAA in the 26-year-old patient (arrows).

tients with GPA or MPA. Therefore, the aim of this retrospective study was to compare a cohort of AAV patients to a sex, age and smoking matched control group for the presence of LAA on HRCT using both visual semi-quantitative and automated quantitative methods. Pulmonary function tests, when available in AAV patients, were assessed for obstructive airway disease and compared to HRCT results.

METHODS

Study Subject Selection

Following approval from our Institutional Review Board (#15-008086) as minimal risk research allowing waiver of informed consent, a total of 751 patients with an AAV diagnosis were identified from the Pulmonary Vasculitis Clinic at the Mayo Clinic Rochester between 2008 and 2015. Filtering for confirmed presence of PR3-ANCA or MPO-ANCA and acquisition of a HRCT between 2008 and 2015, 273 ANCA positive vasculitis patients met study criteria. After screening for subject research authorization approval, the first 100 AAV patients were selected following random number assignment. Study power was determined by estimating a 20% increase in LAA presence on CT for AAV patients compared to control.

For the control cohort, 100 patients from the COPDGene study were selected by 1:1 best fit matching for sex, smoking history and age with weighting based on that order. Asymptomatic non-smokers, asymptomatic smokers and symptomatic smokers with variable degrees obstructive lung disease matched from the COPDGene study composed the control cohort. Regan et al. further outlined the COPDGene study design to include subject selection in 2010 (17).

Imaging Criteria

For subject study inclusion, a volumetric high-resolution chest CT, as defined by contiguous <2mm slice thickness without intravenous contrast reconstructed with high spatial resolution algorithm images, must have been acquired between 2008 and 2015. For the AAV group, all studies were performed at our institution on multidetector scanners for clinically indicated reasons with similar supine full inspiratory imaging acquisition and reconstruction parameters. Specifically, Siemens scans (91 cases) were reconstructed with 1.5mm image thickness at 1.0mm interval using B46f or Bv49 kernel. GE scans (9 cases) were reconstructed with 1.25mm images at 1.0 mm interval using BONE kernel. Eighty-nine were scanned at routine clinical dose, with eleven patients receiving a reduced dose protocol. In the control population, high-resolution CT studies were all performed following COPDGene protocol (17).

Semi-quantitative Visual Analysis

Two subspecialty thoracic radiologists (CWC and BJB) with 10 and 18 years experience, respectively, performed consensus review of all 200 randomly sorted anonymized CT studies blinded to clinical data. Imaging review was performed at our institution PACS workstation on diagnostic grade monitors (EIZO RadiForce RX340) using 4.1v Centricity GE radiology viewing software. Studies were evaluated for presence or absence of visual low attenuation areas (V-LAA) with estimated percent lung involved to the nearest 5%, dominant LAA pattern and distribution. No strict lung density cut-off was applied for the visual assessment, but cumulative changes to include relative decreased density, vascular attenuation, and architectural distortion

all contributed to the interpretation of LAA presence. "Average Percent LAA" represents the mean of percent lung involvement by LAA across the entire population. "Severity Percent LAA" was calculated by averaging the percent of lung involved only in patients with V-LAA present LAA. In the setting of minimal V-LAA, such as a few focal cysts, the distribution was characterized as "scattered". Three or less apical blebs were excluded from V-LAA consideration due to known incidental occurrence in the normal population. V-LAA was subcategorized by the predominant pattern as emphysema (absence of lung parenchyma without definable wall), obstructive (distended lung parenchyma and/or attenuated vasculature with associated relative decrease in lung density), or cystic (absence of lung parenchyma with evident thin wall). CT studies were also evaluated for alternative dominant pulmonary parenchymal patterns of disease. When appropriate, additional characteristics were noted such as 2017 Fleischner Society UIP CT pattern categorization of pulmonary fibrosis (18). Additional acquisitions, such as expiratory imaging, and multi-planar reformatting were not included to maintain consistency across the study groups.

Quantitative Analysis

Using Computer-Aided Lung Informatics for Pathology Evaluation and Rating (CALIPER) automated analysis as previously described (19), all HRCT imaging was analyzed for multiple quantifiable characteristics, to include but not limited to Total Lung Volume, E-950, and texture/density features including quantitative low attenuation areas (Q-LAA), honeycombing, reticulation, ground-glass opacities and pulmonary vascular related structures (PVRS). Quantified absolute values were then converted into percent values relative to the total lung volume. Fibrosing Interstitial Pneumonia (FIP) was calculated by combining the CALIPER values for "Honeycombing" and "Reticulation". The extent of CALIPER-detected "Moderate Q-LAA" and "Severe Q-LAA" were combined to calculate the "Total Q-LAA" volume. To determine the "presence" or "absence" from the quantitative data, a threshold value equal to or greater than 5% was used for the percent E-950 and Total Q-LAA volume, and value equal to or greater than 1% for FIP.

Additional Diagnostic Testing and Mortality Data

In the study cohort, 88 out of 100 AAV patients underwent prior pulmonary function testing (Table 1). In contrast, all 100 control patients underwent pulmonary function testing as part of the COPDGene study (20). Pulmonary function calculations of obstruction were based on the Third National Health and Nutrition Examination Survey reference values with all patients demonstrating obstruction divided into categories of mild, moderate and severe. Chart review was performed on all AAV subjects with alpha-1 antitrypsin deficiency results recorded. Patient mortality through 12/31/2017 was recorded from the institution electronic medical record for AAV subjects and reported from the COPDGene study.

Statistical Analysis

Descriptive statistics are presented as n (%) or mean (standard deviation). The rates or presence of categorical variables between matched AAV patients and controls were compared using McNemar tests. Quantitative variables were compared using paired t-tests or paired Wilcoxon rank sum tests. Agreement is described with kappas for present/absence, or intraclass correlations (ICCs) for quantitative agreement. Mortality risk was compared using univariate and multivariable Cox Proportional Hazard models. Age, gender, LAA, smoking status and packs per year were considered as confounders. Analyses were conducted using SAS (version 9.4; Cary, NC).

RESULTS

Study Subject Selection

Table 1 summarizes the demographic data of both AAV and control cohorts. Ages ranged from 45 to 79 years old in COPDGene study, resulting in 18 AAV subjects younger than 45 years old and 9 AAV subjects greater than 79 years old.

Semi-quantitative Visual Analysis

On semi-quantitative visual inspection of high-resolution chest CT, 46% (46/100) AAV pa-

Table 1. Study Subject Demographics

	AAV Cohort (n=100)	Control Co- hort (n=100)
Mean Age in Years (Range, SD)	59.4 (17-86, 16.7)	61.9 (45-79, 9.7)
Gender		
Female	43**	43
Male	57	57
Prior/Current Smokers	35	35
Mean Packs/Year (\pm SD)	10.7 (\pm 16.9)	10.7 (\pm 16.9)
AAV Subtype		
PR3 Positive	63	N/A
MPO Positive	37	N/A
PFT Performed	88	100

*Unless noted as a mean with standard deviation (SD), all values are absolute

†Absolute values are equal to percent, given cohort populations of 100

AAV=ANCA-Associated Vasculitis, PFT=Pulmonary Function Test

tients demonstrate visual low attenuation areas (V-LAA) compared to 25% (25/100) control patients ($p=0.0017$) although collectively, AAV patients averaged a similar average percent of lung involvement by V-LAA compared to the control cohort (10.0% and 9.1%, respectively, $p=0.7518$). When considering semi-quantitative evaluation of V-LAA severity, severity of V-LAA is statistically significantly greater in controls compared to AAV patients ($p=0.0331$). With respect to subtypes, V-LAA appeared predominantly obstructive ($n=24$, 52%) in AAV, where V-LAA in the control cohort appeared predominantly emphysematous ($n=20$, 80%). Figure 2 provides an example of a young non-smoker with substantial V-LAA characterized a predominantly obstructive. A summary of the V-LAA scoring and quantitative analysis is provided in Table 2. V-LAA in both groups was most often upper lung predominant or diffuse. When categorized as “emphysema”, AAV patients tended to demonstrate a centrilobular pattern. Dividing the AAV patients by PR3 and MPO subgroups, no statistical difference was present with respect to V-LAA with 46% (29/63) PR3-ANCA patients and 46% (17/37) MPO-ANCA patients demonstrating presence of V-LAA ($p=0.9934$).

Considering only the 65 non-smoking AAV patients, semi-quantitative visual inspection reveals

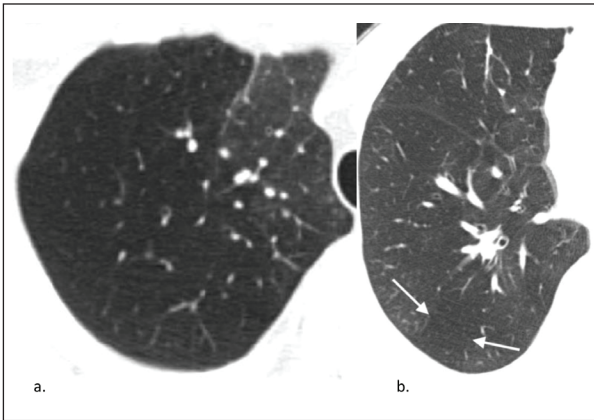


Fig. 2. 36-year-old PR3 positive AAV male (a) and 60-year-old MPO positive female (b), both non-smokers. Select axial HRCT images in lung window reveal low attenuation areas categorized as “obstructive” involving the majority of the right upper lobe in 36-year-old male. More regional areas of obstruction (arrows) are present in the 60-year-old female.

a greater statistically significant difference in AAV patients with V-LAA (n=25, 38%) compared to the non-smoking control patients (n=3, 5%) ($p<0.0001$). A predominantly mosaic appearance of the V-LAA persisted in the non-smoking AAV patients (n=18, 72%), where all 3 non-smoking control patients demonstrated a cystic appearance.

Table 3 summarizes alternative pulmonary parenchymal findings to low-attenuation changes, such as pulmonary fibrosis and nodularity. Visual assessment reveals statistically significant presence of pulmonary fibrosis in AAV patients compared to control (n=34 and 5, respectively, $p<0.0001$), with 8 vasculitis patients demonstrating a “consistent with” or “probable” UIP CT pattern by 2017 Fleischner Society Criteria, compared to none in the control group. With respect to PR3/MPO status, 49% (18/37) MPO positive patients demonstrate fibrosis with 25% (16/63) PR3 patients demonstrating fibrosis. The presence of “nodules”, “groundglass” and “consolidation” were also statistically significantly greater in AAV patients compared to control ($p=0.0027$, $p=0.0001$, $p<0.0001$, respectively). Alternatively, visual HRCT findings of an “airway pattern” to include bronchial wall thickening and/or centrilobular groundglass nodularity was greater in the control group compared to vasculitis patients (43 and 28, respectively, $p=0.0431$) with centrilobular groundglass nodules perceived in 23 non-smoking control patients.

Quantitative Analysis

Quantitative presence of low attenuation areas as measured by $>5\%$ e-950 also demonstrates statistically significant higher rates in AAV patients compared to control, 36% (36/100) AAV to 19% (19/100) control patients ($p=0.0065$). The difference in average percent of e-950 in AAV versus control is similar, with statistically significant greater average e-950 in non-smoking AAV patients compared to the non-smoking control patients ($p=0.0018$). CALIPER textural analysis of quantitative low attenuation areas (Q-LAA) results in no significant difference between AAV and control patients, although percent involvement by Q-LAA in controls was statistically greater than in AAV patients ($p=0.0053$) (Table 2). With regards to fibrotic interstitial lung disease (ILD) as assessed by combining honeycombing and reticulation textural patterns, quantitative analysis also reveals statistically significant greater presence and average percent involvement in AAV compared to controls (both $p<0.0001$) (Table 3). Of note, presence and average percent vessel volume also demonstrate statistically significant greater values in AAV ($p<0.0001$ and $p=0.0032$, respectively). An example CALIPER 3D reconstruction and glyph is provided of a select AAV patient with substantial LAA changes. (Figure 2)

When comparing agreement between obstructive disease CT metrics, e-950 and visual LAA resulted in 68.0% agreement ($\kappa=0.264$, 0.125 to 0.403 95% CI).

Pulmonary Function and Laboratory Testing

Similar to visual and automated e-950 analysis for LAA, pulmonary function tests (PFT) also demonstrate statistically significant greater obstructive lung disease in AAV compared to controls ($p=0.002$), attributable entirely to the difference between non-smoking subgroups (Table 4). In the non-smoking subgroup, PFT values in AAV demonstrate significant obstruction in 35.7% (20/56) of patients. In the smoking subgroup, evidence of obstruction and severity are slightly greater in control patients relative to AAV patients. When comparing agreement between visual presence of LAA, quantitative presence of $>5\%$ e-950, and PFT obstruction, greatest agreement is present between visual LAA and PFT obstruction

Table 2. Visual Semi-quantitative and Automated Quantitative HRCCT Analysis Results for Low Attenuation Changes; AAV versus Control further divided by smoking status

	Smoking		p-value	Nonsmoking		p-value	Total		p-value
	AAV	Controls		AAV	Controls		AAV	Controls	
	n=35	n=35		n=65	n=65		n=100	n=100	
Visual Analysis (V-LAA)									
Presence	21 (60.0%)	22 (62.9%)	0.8084	25 (38.5%)	3 (4.6%)	<0.0001	46 (46.0%)	25 (25.0%)	0.0017
Avg %	11.9% (19.8%)	25.7% (30.6%)	0.0213	8.8% (16.0%)	0.2% (0.9%)	<0.0001	10.0% (17.4%)	9.1% (21.7%)	0.7518
Severity %	19.9% (22.3%)	40.9% (29.4%)	0.0119	23.1% (18.5%)	4.2% (1.4%)	<0.0001	21.6% (20.1%)	36.5% (30.1%)	0.0331
Subtype V-LAA									
Emphysema	11 (52.4%)	20 (90.9%)	0.0068	4 (16.0%)	0	1	15 (32.6%)	20 (80.0%)	0.0001
Obstructive	6 (28.6%)	2 (9.1%)	0.1324	18 (72.0%)	0	0.0366	24 (52.2%)	2 (8.0%)	0.0002
Cysts	5 (23.8%)	2 (9.1%)	0.2404	5 (20.0%)	3 (100.0)	0.0171	10 (21.7%)	5 (20.0%)	0.8639
Automated Analysis									
Avg e-950	408.0 (656.8)	471.5 (641.5)	0.6198	195.5 (221.8)	118.9 (148.8)	0.0253	269.9 (436.3)	242.3 (429.2)	0.5787
Avg % e-950 TV	6.5% (8.7%)	6.6% (8.4%)	0.9429	3.9% (3.8%)	2.0% (2.4%)	0.0018	4.8% (6.1%)	3.7% (5.8%)	0.0994
>5% e-950	15 (42.9%)	12 (34.3%)	0.4054	21 (32.3%)	7 (10.8%)	0.006	36 (36.0%)	19 (19.0%)	0.0065
Avg Total Q-LAA	543.2 (1022.6)	1159.4 (1650.6)	0.0621	239.4 (409.7)	453.3 (818.8)	0.0376	345.7 (699.2)	700.4 (1218.0)	0.0053
Avg % Q-LAA TV	8.3% (13.9%)	16.0% (21.8%)	0.055	4.6% (7.1%)	7.3% (12.7%)	0.1472	5.9% (10.1%)	10.3% (16.9%)	0.0158
Q-LAA Presence	22 (62.9%)	27 (77.1%)	0.1317	31 (52.3%)	39 (60.0%)	0.3532	56 (56.0%)	66 (66.0%)	0.1138

AAV= ANCA-associated Vasculitis, V-LAA= Visual Low attenuation area, Avg= Average, TV= Total Volume, Q-LAA= Quantitative Low attenuation area

Table 3. Visual Semi-quantitative and Automated Quantitative HRCT Analysis Results for Alternative Pulmonary Changes; AAV versus Control further divided by smoking status

	Smoking		p-value	Nonsmoking		p-value	Total	
	AAV	Controls		AAV	Controls		AAV	Controls
	n=35	n=35		n=65	n=65		n=100	n=100
Visual Analysis								
Fibrosis	10 (28.6%)	4 (11.4%)	0.0578	24 (36.9%)	1 (1.5%)	<0.0001	34 (34.0%)	5 (5.0%)
Airway	8 (22.9%)	14 (40.0%)	0.1336	20 (3.08%)	29 (44.6%)	0.1495	28 (28.0%)	43 (43.0%)
Nodularity	0	0	-	1 (1.5%)	0	-	1 (1.0%)	0
Nodules	4 (11.4%)	1 (2.9%)	0.1797	11 (16.9%)	2 (3.1%)	0.0067	15 (15.0%)	3 (3.0%)
Cavities	1 (2.9%)	0	-	2 (3.1%)	0	-	3 (3.0%)	0
Groundglass	4 (11.4%)	2 (5.7%)	0.4142	18 (27.7%)	1 (1.5%)	<0.0001	22 (22.0%)	3 (3.0%)
Consolidation	2 (5.7%)	0	-	9 (13.8%)	0	0.9924	11 (11.0%)	0
Septal Thick	0	0	-	1 (1.5%)	0	-	1 (1.0%)	0
DPO	0	0	-	1 (1.5%)	0	-	1 (1.0%)	0
Automated Analysis								
HC Presence	2 (5.7%)	0	-	5 (7.7%)	0	-	7 (7.0%)	0
Avg FIP % TV	4.5% (8.0%)	1.0% (2.3%)	0.02	6.5% (10.8%)	0.8% (1.8%)	0.0001	5.8% (9.9%)	0.9% (2.0%)
FIP Presence	19 (54.3%)	7 (20.0%)	0.003	35 (53.9%)	11 (16.9%)	<0.0001	54 (54.0%)	18 (18.0%)
Avg Vess Vol	122.5 (58.7)	106.2 (25.2)	0.1229	107.6 (42.7)	92.7 (20.7)	0.0083	112.8 (49.1)	97.4 (23.2)
APVV	2.59% (1.67%)	1.82% (0.5%)	0.0135	2.56% (1.25%)	1.78% (0.34%)	<0.0001	2.57% (1.40%)	1.79% (0.38%)
>3% APVV	6 (17.1%)	1 (2.8%)	0.0379	15 (23.1%)	0	<0.0001	21 (21.0%)	1 (1.0%)

AAV= ANCA-associated Vasculitis, DPO= Diffuse Pulmonary Ossification, TV= Total Volume, HC= Honeycombing, FIP= Fibrosing Interstitial Pneumonia, Vess Vol= Vessel Volume, APVV= Average Percent Vessel Volume

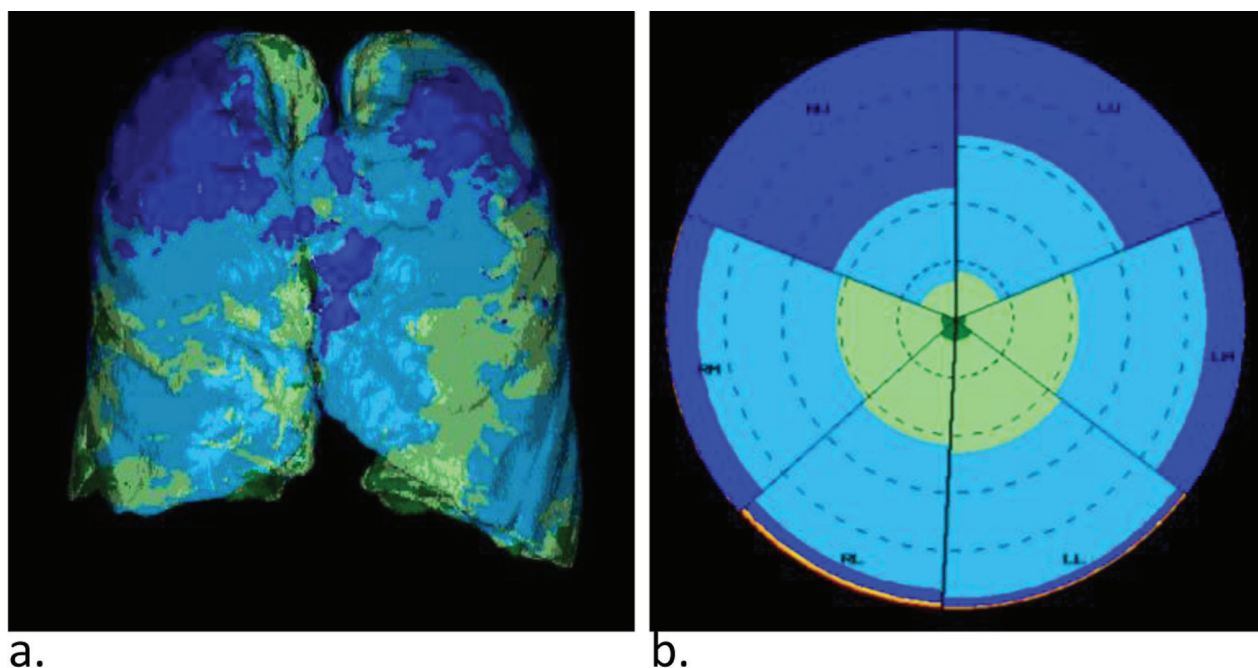


Fig. 3. 75-year-old male smoker with PR3 positive ANCA-associated vasculitis. CALIPER surface rendering (a) and glyph (b) demonstrate significant moderate (light blue) and severe (dark blue) textural low attenuation areas

Table 4. Pulmonary Function Test (PFT) Results, ANCA-associated Vasculitis (AAV) versus Control further divided by smoking status

	Smoking		p-value	Nonsmoking		p-value	Total		p-value
	AAV	Controls		AAV	Controls		AAV	Controls	
	n=35	n=35		n=65	n=65		n=100	n=100	
PFT Results	31	35		56	65		87	100	
Obstruction	12 (38.7%)	17 (48.6%)	0.593	20 (35.7%)	0	<0.0001	32 (36.8%)	17 (17.0%)	0.002
Severity			0.1302			-			0.1744
Mild	1 (8.3%)	5 (29.4%)		3 (15.8%)	0		4 (12.9%)	5 (29.4%)	
Moderate	7 (58.3%)	4 (33.3%)		8 (42.1%)	0		15 (48.4%)	4 (23.5%)	
Severe	4 (33.3%)	8 (47.1%)		8 (42.1%)	0		12 (38.7%)	8 (47.1%)	

(Kappa 0.509, 0.377 to 0.641 95% CI and 79.1% agreement). Alpha-1 Antitrypsin Deficiency testing was performed on 6 AAV patients, all negative.

Mortality

All-cause mortality between AAV and control patients was not statistically different, 12 compared to 8, respectively (HR (95% CI): 2.33 (0.92, 5.90),

$p=0.0729$). Age and gender were also significantly associated with mortality risk after adjusting for AAV (males HR (95% CI): 2.93 (1.12, 7.69, $p=0.029$; age HR (95% CI): 1.10 (1.05, 1.16), $p=0.0002$). Across the entire study population, V-LAA demonstrated the greatest association with mortality ($p=0.0085$), but was not significant after adjusting for age, gender, and AAV. Total population mortality results are summarized in Table 5.

Table 5. All-Cause Mortality Comparisons and Cox Proportional Hazard Model results

	Mortality		HR (95% CI)	p-value
	Yes (n=20)	No (n=180)		
<u>Study Group</u>				
AAV Subjects	12 (12.0%)	88 (88.0%)	1.97 (0.80, 4.87)	0.1402
Control Subjects	8 (8.0%)	92 (92.0%)		
<u>Gender</u>				
Male	14 (16.3%)	72 (83.7%)	3.19 (1.23, 8.31)	0.0174
Female	6 (5.3%)	108 (94.7%)		
<u>Visual Assessment</u>				
V-LAA- yes	13 (18.3%)	58 (81.7%)	3.43 (1.37, 8.61)	0.0085
V-LAA- no	7 (5.4%)	122 (94.6%)		
<u>Quantitative Assessment</u>				
Adj e950 >5%	7 (12.7%)	48 (87.3%)	1.56 (0.62, 3.91)	0.3440
Adj e950 <5%	13 (9.0%)	132 (91.0%)		
<u>Pulmonary Function Test</u>				
Obstruction	7 (14.6%)	41 (85.4%)	2.24 (0.88, 5.68)	0.0891
No obstruction	11 (7.9%)	128 (92.1%)		
<u>Multivariable Cox PH Model</u>	HR	95% CI		Adjusted p-value
Age	1.10	1.05, 1.16		0.0002
Gender (M)	2.93	1.12, 7.69		0.0290
AAV	2.33	0.92, 5.90		0.0729

AAV= ANCA-associated Vasculitis, V-LAA= Visual Low attenuation areas

DISCUSSION

Overall, visual semi-quantitative analysis of high-resolution chest CT for pulmonary low attenuation areas (V-LAA), automated quantitative analysis for e-950, and obstruction on pulmonary function testing are statistically significantly greater in ANCA-associated vasculitis (AAV) patients when compared to age, gender and smoking matched controls. V-LAA in AAV subjects compared to the control group demonstrated the greatest difference between the populations. With respect to a unique pattern of low attenuation area for AAV patients, only one AAV patient and no control patients demonstrated the described emphysematous changes tracking

along bronchovascular bundles, suggesting that this is a unique pattern to AAV, albeit rare.

While association does not prove causality, there are potential inflammatory mechanisms for development of low attenuation areas on CT imaging and/or functional obstructive lung disease in the setting of ANCA-associated vasculitis. Complex inflammatory pathways play a primary role in the development of chronic obstructive pulmonary disease, to include but not limited to an initial trigger, such as smoking, leading to a diverse cellular response with subsequent tissue damage, release of inflammatory mediators and cellular activation for a mixed cellular inflammatory milieu. Final inflammatory cascades result in protease/antiprotease imbalance, increased oxidative

stress and altered lung cell death resulting in COPD (21). Likewise, pulmonary AAV inflammatory cascades overlap with these known COPD pathways, particularly neutrophil and T cell activation causing direct injury to the lung (22,23).

A correlated alternative pathologic process in AAV, such as alpha-1 antitrypsin deficiency (AATD), may be causing the difference in low attenuation areas on chest CT and physiologic obstructive lung disease. Presence of AATD genetic alleles is known to increase in the setting of AAV (24). Despite only 6 patients out of 100 AAV patients being tested for AATD, all AAV patients tested were negative for AATD.

When examining the study subgroups, a few specific differences stand out. First, the difference in V-LAA between AAV and control groups was entirely found in the nonsmoking subgroup. Another interesting difference is evident when comparing smokers, where AAV subjects demonstrated a slight decrease in V-LAA presence and a statistically significant decrease in V-LAA severity compared to control subjects who smoke. Mild V-LAA was present in 3% of control non-smokers, all of which were over the age of 70 years old, similar to other study findings of senescent changes of the lung (25).

Studies using CALIPER for quantitative CT analysis have demonstrated better correlation between textural quantitative low attenuation area measurements and obstructive physiology on pulmonary function testing when compared to visual assessment (26) as well as comparable performance of CALIPER measurements to physiologic testing (27). In our study, CALIPER analysis of textural quantitative low attenuation areas (Q-LAA) modeled on emphysema measured greater areas of moderate and severe Q-LAA in controls as opposed to AAV, which runs counter to the other CT and physiologic obstruction metrics. Agreement between V-LAA, e-950 and obstructive lung disease on PFTs favors the textural analysis for Q-LAA as the outlier. Since most subjects have mild V-LAA and some have additional airway features such as bronchial wall thickening or centrilobular nodules that increase density, the combination of minimal lucency and some small high-density features in the VOI likely result in CALIPER under-detecting the subtle features which are captured by pixel-counting and expert visual review. This may also explain the divergence of

Q-LAA performance in our study on vasculitis when compared to the findings of Jacob et al. in the setting of hypersensitivity pneumonitis (26). Furthermore, the pattern of AAV low attenuation areas is visually different than typical smoking-related emphysema, with many subtyped as obstructive pattern. As CALIPER was trained with pathologically proven emphysema datasets, the under-detection of the AAV low attenuation areas is not entirely surprising.

The prevalence of obstructive disease in the setting of AAV varies in the literature depending on the metric. A recent evaluation of HRCT findings in patients from the Remission Induction Therapy in Japanese Patients With ANCA-Associated Vasculitis and Rapidly Progressive Glomerulonephritis Study, Suzuki et al. found emphysema in 22% of patients with another 7% demonstrating mosaic attenuation (16). Greenan et al found a relatively similar rate of 25.9% of chest CT revealing emphysema in AAV patients (9). When examining pulmonary function testing in AAV, Newall et al. found obstructive airway disease in 12 out of 30 AAV patients (40%) (28). In our study, prevalence of finding suggesting obstructive airway disease on visual HRCT analysis, quantitative HRCT analysis and pulmonary function tests ranged from 36% to 46%, which likely reflects the more general assessment for LAA identifying mosaic attenuation as a subset of obstruction in addition to emphysema on CT and better correlating with reported obstructive disease on PFT. Additional contributors may include selection bias related to increased disease severity, comorbidities or treatment differences.

Treatment of airway obstruction in AAV patients is based on clinical symptoms paired with PFT abnormalities following guidelines for COPD management. The radiographic observations in our study may in part explain clinical symptoms and PFT abnormalities in patients with ANCA-associated vasculitis that cannot be explained based on smoking history.

Outside of obstructive changes, pulmonary fibrosis was also increased in AAV patients on both visual and automated analysis compared to controls. In keeping with multiple prior studies and reports, MPO/MPA AAV patients demonstrated greater prevalence of fibrosis, although proportionally were higher at 51%. PR3/GPA patients also demonstrated increased prevalence of pulmonary fibrosis at 24%.

Automated quantitative analysis measured even greater differences of pulmonary fibrosis in AAV compared to controls to include smokers and nonsmokers. Pulmonary fibrosis may confound evaluation of obstructive airway disease in both HRCT and PFT.

Beyond retrospective design, there were a few known limitations to the study. The AAV study population was selected from a quaternary referral center, which may represent a more complicated or atypical subpopulation. Studying AAV patients with prior chest CT introduces selection bias for those having clinical indications for CT such as respiratory symptoms. Not all AAV patients underwent pulmonary function testing could artificially increase the percent demonstrating obstruction. Mortality rates were generally low, and therefore comparisons of potential mortality risks were underpowered. Control subjects were collected as part of a multicenter trial across the country and may not reflect an ideal equivalent control population. In particular, the COPDGene study design included a distribution of two-thirds Non-Hispanic white and one-third African American, which is quite different than the more homogeneously non-Hispanic white cohort of AAV subjects studied.

Pulmonary low attenuation areas on visual and quantitative HRCT analysis, as opposed to narrower imaging definitions of emphysema, in AAV patient better correlates with prevalence of obstruction on pulmonary function testing. In our study, visual low attenuation areas correlated best with obstructive lung disease (79.1% agreement), although establishing quantitative measures of LAA on HRCT in the setting of AAV provides a standard to judge disease severity and track progression. These advances in pulmonary imaging assessment in AAV patients may improve diagnostic categories and may even assist in guiding treatment. Future studies focused on obstructive lung disease in the setting of AAV should consider temporal evolution of disease relative to disease onset, type and severity, development and response of obstructive disease CT findings related to treatment, and further classification of LAA HRCT findings by histopathology correlation.

ACKNOWLEDGEMENTS

This study was approved as an ancillary study (ANC243) to the COPDGene study.

REFERENCES

1. Fries JF, Hunder GG, Bloch DA et al. The American College of Rheumatology 1990 criteria for the classification of vasculitis. Summary. *Arthritis Rheum* 1990 Aug; 33(8): 1135-6.
2. Jennette JC, Falk RJ, Bacon PA et al. 2012 Revised International Chapel Hill Consensus Conference Nomenclature of Vasculitides. *Arthritis Rheum* 2013 Jan; 65(1): 1-11.
3. Bossuyt X, Cohen Tervaert J, Arimura Y et al. Revised 2017 international consensus on testing of ANCA in granulomatosis with polyangiitis and microscopic polyangiitis. *Rheumatology* 2017 Nov; 13: 683-92.
4. Brown KK. Pulmonary Vasculitis. *Proc Am Thorac Soc* 2006; 3:48-57.
5. Mahmoud S, Ghosh S, Farver C et al. Pulmonary Vasculitis Spectrum of Imaging Appearances. *Radiol Clin N Am* 2016; 54:1097-1118.
6. Castaner E, Alguersuari A, Andreu M et al. Imaging Findings in Pulmonary Vasculitis. *Semin Ultrasound CT MRI* 2012; 33:567-579.
7. Hervier B, Pagnoux C, Agard C et al. Pulmonary fibrosis associated with ANCA-positive vasculitides. Retrospective study of 12 cases and review of the literature. *Ann Rheum Dis* 2009; 68:404-407.
8. Greenan K, Vassallo D, Chinnadurai et al. Respiratory manifestations of ANCA-associated vasculitis. *Clin Respir J* 2018; 12:57-61.
9. Foulon G, Delaval P, Valeyre D et al. ANCA-associated lung fibrosis: Analysis of 17 patients. *Respiratory Medicine* 2008; 102:1392-1398.
10. Tzelepis GE, Kokosi M, Tzioufas A et al. Prevalence and outcome of pulmonary fibrosis in microscopic polyangiitis. *Eur Respir J* 2010; 36:116-121.
11. Comarmond C, Bruno C, Abdellatif T et al. Pulmonary Fibrosis in Antineutrophil Cytoplasmic Antibodies (ANCA)-Associated Vasculitis: A Series of 49 Patients and Review of the Literature. *Medicine* 2014; 93:340-349.
12. Mohammad AJ, Mortensen KH, Babar J et al. Pulmonary Involvement in Antineutrophil Cytoplasmic Antibodies (ANCA)-associated Vasculitis: The Influence of ANCA Subtype. *J Rheumatol* 2017; 44:1458-1467.
13. Pujara AC and Mohammed TH. Hypocomplementemic Urticarial Vasculitis Syndrome: A Rare Cause of Basilar Panacinar Emphysema. *J Thorac Imaging* 2012; 27:W50-W51.
14. Schwarz MI, Mortenson RL, Colby TV et al. Pulmonary Capillaritis: The Association with Progressive Irreversible Airflow Limitation and Hyperinflation. *Am Rev Respir Dis* 1993; 148:507-511.
15. Gadre SK, Stoller JK and Mehta AC. Granulomatosis with polyangiitis and associated pulmonary emphysema: Breathtaking vasculitis. *Lung India* 2015; 32:367-369.
16. Suzuki A, Sakamoto S, Kurosaki A et al. Chest High-Resolution CT Findings of Microscopic Polyangiitis: A Japanese First Nationwide Prospective Cohort Study. *AJR* 2019; 213: 104-114.
17. Regan EA, Hokanson JE, Murphy JR et al. Genetic Epidemiology of COPD (COPDGene) Study Design. *COPD* 2010; 7(1): 32-43.
18. Lynch DA, Sverzellati N, Travis WD et al. Diagnostic criteria for idiopathic pulmonary fibrosis: a Fleischner Society White Paper. *Lancet Respir Med* 2018; 6(2): 138-153.
19. Jacob J, Bartholmai BJ, Rajagopalan S et al. Automated Quantitative Computed Tomography Versus Computed Tomography Scoring in Idiopathic Pulmonary Fibrosis. *J Thorac Imaging* 2016; 31(5):304-311.
20. Kinney GL, Santorico SA, Young KA et al. Identification of Chronic Obstructive Pulmonary Disease Axes That Predict All-Cause Mortality The COPDGene Study. *Am J Epidemiol* 2018; 187(10):2109-2116.
21. Cornwell WD, Kim V, Song C and Rogers TJ. Pathogenesis of Inflammation and Repair in Advanced COPD. *Semin Respir Crit Care Med* 2010; 31(3):257-266.
22. Cartin-Ceba R, Peikert T and Specks U. Pathogenesis of ANCA-Associated Vasculitis. *Rheum Dis Clin North Am* 2010; 36(3):463-477.

23. Alba MA, Jennette JC and Falk RJ. Pathogenesis of ANCA-Associated Pulmonary Vasculitis. *Semin Respir Crit Care Med* 2018; 39:413-424.
24. Mahr AD, Edberg JC, Stone JH et al. Alpha1-Antitrypsin Deficiency-Related Alleles Z and S and the Risk of Wegener's Granulomatosis. *Arthritis Rheum* 2010; 62(12):3760-3767.
25. Copley SJ, Wells AU, Hawtin KE et al. Lung Morphology in the Elderly: Comparative CT Study of Subjects over 75 Years Old versus Those under 55 Years Old. *Radiology* 2009; 251(2):566-573.
26. Jacob J, Bartholmai B, Brun AL et al. Evaluation of visual and computer-based CT analysis for the identification of functional patterns of obstruction and restriction in hypersensitivity pneumonitis. *Respirology* 2017; 22(8):1585-1591.
27. Matsumoto AJ, Bartholmai B and Wylam ME. Comparison of Total Lung Capacity Determined by Plethysmography with Computed Tomographic Segmentation Using CALIPER. *Journal of Thoracic Imaging* 2017; 32(2):101-106.
28. Newall C, Schinke S, Savage CO et al. Impairment of lung function, health status and functional capacity in patients with ANCA-associated vasculitis. *Rheumatology* 2005; 44:623

COPDGene Phase 3

Grant Support and Disclaimer

The project described was supported by Award Number U01 HL089897 and Award Number U01 HL089856 from the National Heart, Lung, and Blood Institute. The content is solely the responsibility of the authors and does not necessarily represent the official views of the National Heart, Lung, and Blood Institute or the National Institutes of Health.

COPD Foundation Funding

The COPDGene® project is also supported by the COPD Foundation through contributions made to an Industry Advisory Board comprised of AstraZeneca, Boehringer Ingelheim, GlaxoSmithKline, Novartis, Pfizer, Siemens and Sunovion.

COPDGene® Investigators – Core Units

Administrative Center: James D. Crapo, MD (PI); Edwin K. Silverman, MD, PhD (PI); Barry J. Make, MD; Elizabeth A. Regan, MD, PhD

Genetic Analysis Center: Terri Beaty, PhD; Ferdouse Begum, PhD; Peter J. Castaldi, MD, MSc; Michael Cho, MD; Dawn L. DeMeo, MD, MPH; Adel R. Boueiz, MD; Marilyn G. Foreman, MD, MS; Eitan Halper-Stromberg; Lystra P. Hayden, MD, MMSc; Craig P. Hersh, MD, MPH; Jacqueline Hetmanski, MS, MPH; Brian D. Hobbs, MD; John E. Hokanson, MPH, PhD; Nan Laird, PhD; Christoph Lange, PhD; Sharon M. Lutz, PhD; Merry-Lynn McDonald, PhD; Margaret M. Parker, PhD; Dandi Qiao, PhD; Elizabeth A. Regan, MD, PhD; Edwin K. Silverman, MD, PhD; Emily S. Wan, MD; Sungho Won, Ph.D.; Phuwanat Sakornsakolpat, M.D.; Dmitry Prokopenko, Ph.D.

Imaging Center: Mustafa Al Qaisi, MD; Harvey O. Coxson, PhD; Teresa Gray; MeiLan K. Han, MD, MS; Eric A. Hoffman, PhD; Stephen Humphries, PhD; Francine L. Jacobson, MD, MPH; Philip F. Judy, PhD; Ella A. Kazerooni, MD; Alex Kluiber; David A. Lynch, MB; John D. Newell, Jr., MD; Elizabeth A. Regan, MD, PhD; James C. Ross, PhD; Raul San Jose Estepar, PhD; Joyce Schroeder, MD; Jered Sieren; Douglas Stinson; Berend C. Stoel, PhD; Juerg Tschirren, PhD; Edwin Van Beek, MD, PhD; Bram van Ginneken, PhD; Eva van Rikxoort, PhD; George Washko, MD; Carla G. Wilson, MS;

PFT QA Center, Salt Lake City, UT: Robert Jensen, PhD

Data Coordinating Center and Biostatistics, National Jewish Health, Denver, CO: Douglas Everett, PhD; Jim Crooks, PhD; Camille Moore, PhD; Matt Strand, PhD; Carla G. Wilson, MS

Epidemiology Core, University of Colorado Anschutz Medical Campus, Aurora, CO: John E. Hokanson, MPH, PhD; John Hughes, PhD; Gregory Kinney, MPH, PhD; Sharon M. Lutz, PhD; Katherine Pratte, MSPH; Kendra A. Young, PhD

Mortality Adjudication Core: Surya Bhatt, MD; Jessica Bon, MD; MeiLan K. Han, MD, MS; Barry Make, MD; Carlos Martinez, MD, MS; Susan Murray, ScD; Elizabeth Regan, MD; Xavier Soler, MD; Carla G. Wilson, MS

Biomarker Core: Russell P. Bowler, MD, PhD; Katerina Kechris, PhD; Farnoush Banaei-Kashani, Ph.D

COPDGene® Investigators – Clinical Centers

Ann Arbor VA: Jeffrey L. Curtis, MD; Carlos H. Martinez, MD, MPH; Perry G. Pernicano, MD

Baylor College of Medicine, Houston, TX: Nicola Hanania, MD, MS; Philip Alapat, MD; Mustafa Atik, MD; Venkata Bandi, MD; Aladin Boriek, PhD; Kalpatha Guntupalli, MD; Elizabeth Guy, MD; Arun Nachiappan, MD; Amit Parulekar, MD;

Brigham and Women's Hospital, Boston, MA: Dawn L. DeMeo, MD, MPH; Craig Hersh, MD, MPH; Francine L. Jacobson, MD, MPH; George Washko, MD

Columbia University, New York, NY: R. Graham Barr, MD, DrPH; John Austin, MD; Belinda D'Souza, MD; Gregory D.N. Pearson, MD; Anna Rozenshtein, MD, MPH, FACR; Byron Thomashow, MD

Duke University Medical Center, Durham, NC: Neil MacIntyre, Jr., MD; H. Page McAdams, MD; Lacey Washington, MD

HealthPartners Research Institute, Minneapolis, MN: Charlene McEvoy, MD, MPH; Joseph Tashjian, MD

Johns Hopkins University, Baltimore, MD: Robert Wise, MD; Robert Brown, MD; Nadia N. Hansel, MD, MPH; Karen Horton, MD; Allison Lambert, MD, MHS; Nirupama Putcha, MD, MHS

Los Angeles Biomedical Research Institute at Harbor UCLA Medical Center, Torrance, CA: Richard Casaburi, PhD, MD; Alessandra Adami, PhD; Matthew Budoff, MD; Hans Fischer, MD; Janos Porszasz, MD, PhD; Harry Rossiter, PhD; William Stringer, MD

Michael E. DeBakey VAMC, Houston, TX: Amir Sharafkhaneh, MD, PhD; Charlie Lan, DO

Minneapolis VA: Christine Wendt, MD; Brian Bell, MD

Morehouse School of Medicine, Atlanta, GA: Marilyn G. Foreman, MD, MS; Eugene Berkowitz, MD, PhD; Gloria Westney, MD, MS

National Jewish Health, Denver, CO: Russell Bowler, MD, PhD; David A. Lynch, MB

Reliant Medical Group, Worcester, MA: Richard Rosiello, MD; David Pace, MD

Temple University, Philadelphia, PA: Gerard Criner, MD; David Ciccolella, MD; Francis Cordova, MD; Chandra Dass, MD; Gilbert D'Alonzo, DO; Parag Desai, MD; Michael Jacobs, PharmD; Steven Kelsen, MD, PhD; Victor Kim, MD; A. James Mamary, MD; Nathaniel Marchetti, DO; Aditi Satti, MD; Kartik Shenoy, MD; Robert M. Steiner, MD; Alex Swift, MD; Irene Swift, MD; Maria Elena Vega-Sanchez, MD

University of Alabama, Birmingham, AL: Mark Dransfield, MD; William Bailey, MD; Surya Bhatt, MD; Anand Iyer, MD; Hrudaya Nath, MD; J. Michael Wells, MD

University of California, San Diego, CA: Joe Ramsdell, MD; Paul Friedman, MD; Xavier Soler, MD, PhD; Andrew Yen, MD

University of Iowa, Iowa City, IA: Alejandro P. Comellas, MD; Karin F. Hoth, PhD; John Newell, Jr., MD; Brad Thompson, MD

University of Michigan, Ann Arbor, MI: MeiLan K. Han, MD, MS; Ella Kazerooni, MD; Carlos H. Martinez, MD, MPH

University of Minnesota, Minneapolis, MN: Joanne Billings, MD; Abbie Begnaud, MD; Tadashi Allen, MD

University of Pittsburgh, Pittsburgh, PA: Frank Sciurba, MD; Jessica Bon, MD; Divay Chandra, MD, MSc; Carl Fuhrman, MD; Joel Weissfeld, MD, MPH

University of Texas Health Science Center at San Antonio, San Antonio, TX: Antonio Anzueto, MD; Sandra Adams, MD; Diego Maselli-Caceres, MD; Mario E. Ruiz, MD